Chalcogenide Letters Vol. 18, No. 2, February 2021, p. 59 - 64

IN-SITU TRANSFORMATION INTO $MoSe_2/MoO_x$ HETEROGENEOUS NANOSTRUCTURES WITH ENHANCED TRIBOLOGICAL PERFORMANCE AS LUBRICATION ADDITIVE

G.H.NI*, A.X.PAN, C.Q.WU, F.YUAN, M. XUE*
Changzhou Institute of Industry Technology, Changzhou, Jiangsu 213164, P. R. China

As lubricating materials, the tribological performance of laminar transition metal dichalcogenides (TMDs), can be improved by compound oxide particles. In this study, $MoSe_2/MoO_x$ heterogeneous nanostructures are easily obtained from a solvothermal reaction followed by an annealed process in O_2/N_2 atmosphere. The $MoSe_2/MoO_x$ composite, as a lubricant additive, shows better performance than those of pristine base oil, which includes friction coefficient and antiwear capability. The enhanced performance of $MoSe_2/MoO_x$ heterogeneous nanostructures can be attributed to the lubrication layer and tribochemical reaction films formed on the worn surface, which prevents the direct contact of the friction surface and improves tribological performance.

(Received November 28, 2020; Accepted February 4, 2021)

Keywords: $MoSe_2/MoO_x$, Heterogeneous nanostructures, Solvothermal reaction, Tribological performance

1. Introduction

The rapid development of modern industry, information technology, biomedicine, aerospace and other disciplines, as well as the complexity and diversification of equipment working environment, pose great challenges to the development, preparation and manufacturing of high-performance materials. In this context, traditional lubricants can no longer meet the needs of various complicated environments, therefore, it is urgent to develop a new generation of lubricating oil and lubricant[1-3]. Transition metal sulfides such as Molybdenum disulfide (MoS_2) and Molybdenum disselenide ($MoSe_2$) are widely used as lubricants in various optoelectronic devices, mEMS, lubricating devices, sensors and flexible electronic devices due to their unique characteristics of easy sliding between layers [4-9].

As a typical two-dimensional transition metal dichalcogenides (TMDs) material, molybdenum diselenide ($MoSe_2$) is vertically stacked in sandwiched layers (Se–Mo–Se) with weak interactions [10]. Recent studies have shown that these $MoSe_2$/oxide composites have fargoing applications, Huang et al. reported the synthesis of $SnO_2@MoSe_2$ nanostructure through a facile electrospinning technique combined with sintering and a solvothermal process, and demonstrated that the hydrogen evolution reaction catalytic activity of $MoSe_2$ nanosheets covering on SnO_2 nanotubes correlates directly with the unique hierarchical tubular structure with fully exposed active edges and open spaces [11]. Yang and coworkers successfully prepared porous, conductive and flexible membranes composed of $MoSe_2$ nanosheet/MoO_2 nanobelt/carbon nanotube through a vacuum filtration followed by an annealed process, which enhanced the exposed active sites, thus resulting in remarkable electrocatalytic performance for the HER and excellent long-cycle stability[12]. Kang et al. [13] reported a new type of $MoSe_2$ /MoO_3 heterogeneous nanostructures through a facile solvothermal reaction followed by high-temperature annealing in an inert atmosphere, and found that $MoSe_2/MoO_3$ heterogeneous nanostructure composite as an anode material for SIBs shows better charge/discharge capacity, cycling stability and rate capability. Xue et al. [14] studied the tribological properties of $Cu/MoSe_2/MoO_x$ and

*Corresponding author: 103668561@qq.com
https://doi.org/10.15251/CL.2021.182.59

found that the improved the friction-reducing and anti-wear properties of copper matrix was due to the the synergic effects of the $MoSe_2/MoO_x$ in the nanocomposite structure.

As far as we know, there have been few reports on the tribological performance of $MoSe_2/MoO_x$ as lubrication additive. Herein, we report using an efficient route to prepare a $MoSe_2/MoO_x$ heterogeneous nanostructures. As a result, the obtained $MoSe_2/MoO_x$ had better lubricating properties in base oil. The lubricating mechanism of the as-synthesized $MoSe_2/MoO_x$ was also discussed.

2. Experimental

2.1. $MoSe_2$ and $MoSe_2/MoO_x$ composite synthesis

The chemical reagents used in this work were analytical grade. $MoSe_2$ was prepared using a solvothermal reaction. In a typical process, 0.507 g ammonium molybdate $(NH_4)_2MoO_4\cdot 2H_2O$ and 0.316 g Se powder were added into a mixed solvent (10.0mL hydrazine hydrate $(N_2H_4\cdot H_2O)$ and 60.0 mL deionized water) and stirred for 20 min. The pH value of the mixture was adjusted to 12 by addition of NaOH solution. The above solution was transferred into a Teflon-lined stainless steel autoclave and maintained at 200°C for 48 h. After cooling to room temperature naturally, the obtained precipitate was collected by centrifugation, washed with distilled water and absolute ethanol several times, and dried at 70°C for 12 h. The as-prepared $MoSe_2$ sample was calcinated at 550°C for 30 min. in a mixed O_2/N_2 atmosphere with a heating rate of 10°C/min. After gradual cooling of samples, $MoSe_2$ /MoO_x (x=2,3) composite was obtained.

2.2. Material characterization

The crystal structure of the samples was examined by means of X-ray diffraction (XRD, Shimadzu LabX XRD-6000, Cu-Ka radiation), data analysis with Jade software. The samples were characterized by scanning electron microscope (SEM) JEOL JXA-840A and energy-dispersive spectrometer (EDS).

2.3. Tribological test

The as-prepared $MoSe_2/MoO_x$ samples were ultrasonic dispersion in the base oil without any active reagent. The tribological properties of the samples were investigated using a UMT-2 ball-on-disc tribometer at ambient conditions. The testing of the anti-wear and friction reducing performance was carried out for 800 s. The balls of 10 mm in diameter used in the tests were made of 440C stainless steel with a hardness of 62 HRC. The discs were 45 steel disc (Ø 30 mm × 5 mm). The friction coefficient was recorded automatically by a computer and the wear scars widths (WSW) of the discs were measured with a metallographic microscope. Morphologies of worn surface were analyzed under a scanning electron microscope (SEM, JSM-5600LV).

3. Results and discussions

The preparation process of heterogeneous $MoSe_2/MoO_x$ nanostructure is schematically illustrated in Fig. 1. After a facile solvothermal reaction followed by an annealed process in O_2/N_2 atmosphere. X-ray diffraction (XRD) patterns used to identify the crystal structure and phase purity are shown in Fig. 2a. After calcination in a mixed O_2/N_2 atmosphere, the diffraction peaks are sharp and intensive, indicating high crystallinity. The characteristic peaks are well indexed to $MoSe_2$ (JCPDF 29-0914), MoO_2 (JCPDF 65-5787) and MoO_3 (JCPDF 05-0508). The results indicate that $MoSe_2/MoO_x$ (x=2,3) were successfully fabricated.

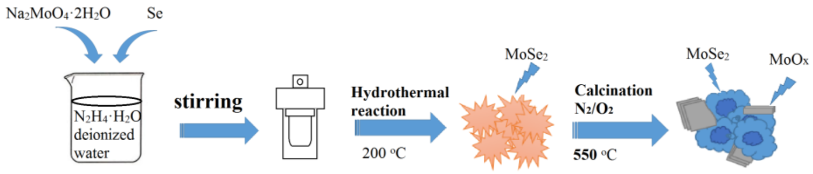

Fig. 1. Schematic diagram of the preparation of heterogeneous $MoSe_2$ /MoO_x nanostructure.

SEM measurements were then carried out to examine the surface morphologies. Fig. 2b depicts an overview of the $MoSe_2$/MoO_x heterogeneous nanostructures, it can be seen that nanostructures composed of many flower-like assemblies with a size of 200-300 nm and aggregated laminated crisp flakes. The magnified SEM image (Fig. 2c, 2d) further gives the details of heterogeneous nanostructures, it can be clearly seen that the thickness of the obtained flakes is about 200 nm, the laminated structure is evident in Fig. 2c. Fig.2d reveals that the flower-like nanostructures is built from a number of curvy nanosheets with the thickness about 20 nm, which are most likely $MoSe_2$ nanosheets compare to the previous literature [15].The elementary composition of the $MoSe_2$/MoO_x heterogeneous nanostructures were also confirmed by Energy-dispersive spectrometer (EDS), as shown in Fig. 2e reveals that the laminated crisp flakes mainly composed of element Mo and O, indicating the synthesis of MoO_x, and the flower-like nanostructures mainly composed of element Mo and Se, indicating the synthesis of $MoSe_2$.

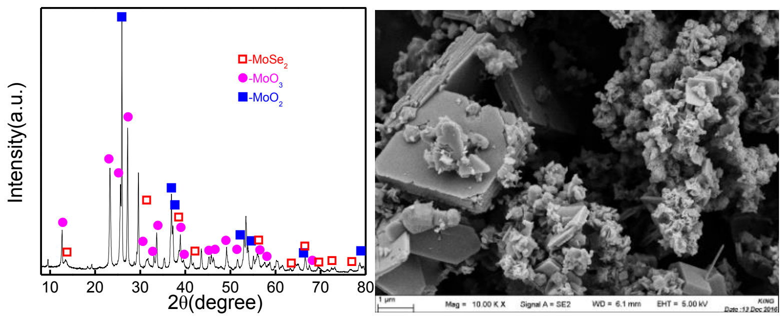

(a) *(b)*

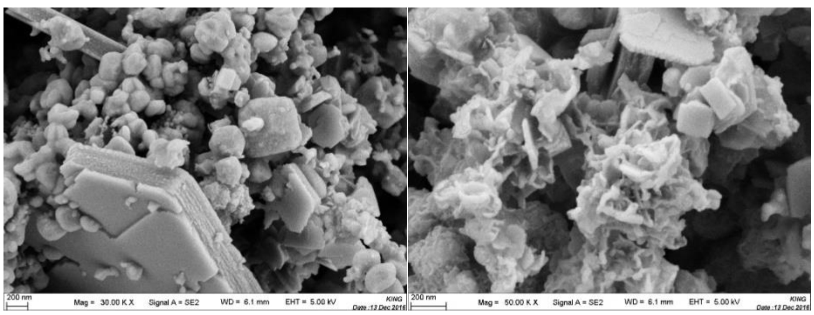

(c) *(d)*

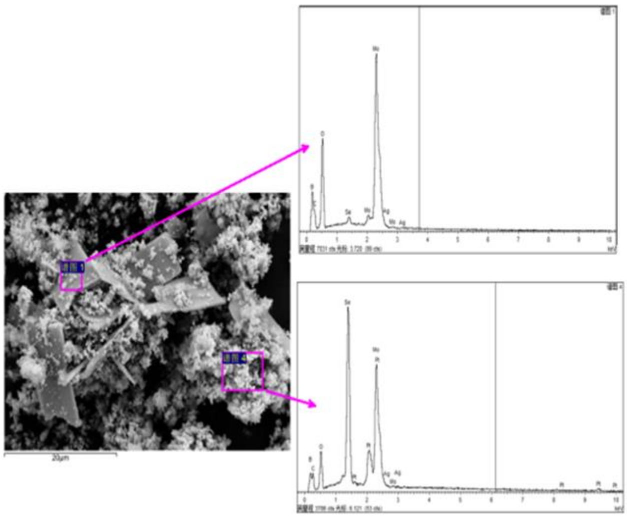

(e)

Fig. 2. (a) XRD pattern, (b)(c)(d) SEM image and (e) EDS of the as-obtained $MoSe_2$.

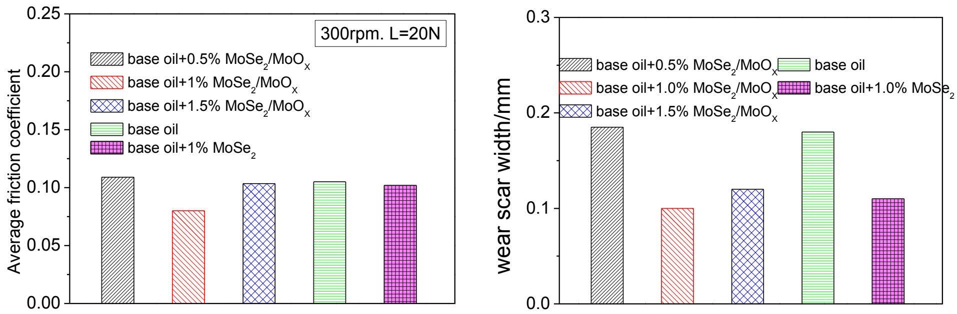

(a) *(b)*

Fig. 3. Variation in tribological properties with increased content of $MoSe_2/MoO_x$ in base oil: (a) friction–time curves and (b) average wear scar diameter.

Fig. 3 shows the variation in tribological properties of base oil with increased addition of $MoSe_2/MoO_x$ heterogeneous nanostructures. The addition of 0.5% $MoSe_2/MoO_x$ did not improve the friction reduction of base oil (Fig. 3a) and even slightly weakened the wear resistance of base oil (Fig. 3b). However, the addition of 1.0% $MoSe_2/MoO_x$ significantly improved the tribological properties of base oil. These results are similar to those reported in Ref. [16]. The two figures also reveal that 1.0% $MoSe_2$ slightly decreased the friction coefficient and remarkably improved the wear resistance of base oil, which is similar to the testing result in liquid paraffin with nano-TiO_2 [10]. Compared with 0.5% $MoSe_2/MoO_x$ and 1.5% $MoSe_2/MoO_x$, the 1.0% $MoSe_2/MoO_x$ presented better friction reduction in base oil. Moreover, the wear resistance of the 1.0% $MoSe_2/MoO_x$ remarkably exceeded that of the other additives.

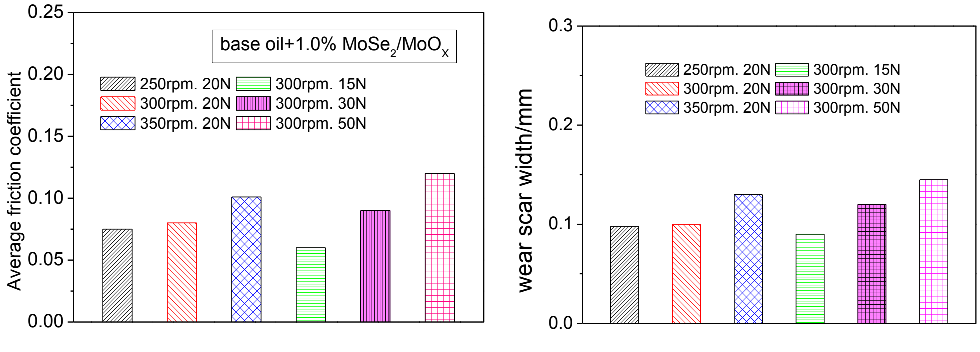

(a) *(b)*

Fig. 4. Variation in the tribological properties of 1.0% $MoSe_2/MoO_x$ in base oil with increased load and sliding velocity: (a) friction–time curves and (b) average wear scar width.

Fig.4 provides the variation in the tribological properties of base oil with increased load and sliding velocity. The friction coefficient increased with increased sliding velocity and load. The wear presented a similar variation trend.

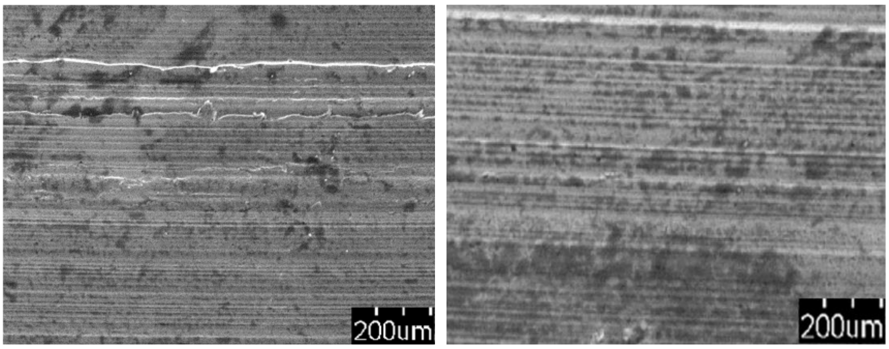

(a) *(b)*

Fig. 5. SEM on the selected typical friction lubricated by (a) base oil and (b)base oil with 1.0 wt% $MoSe_2/MoO_x$ at 300rpm.

Fig. 5 shows the SEM images wear scars on the disc lubricated by base oil with or without 1.0 wt% $MoSe_2/MoO_x$ at 300 rpm. for 800s. As shown in the figure, grooves can be observed in both micrographs, indicating that the abrasive wear is a major mode of the disk. However, the abrasive plowing differed from each friction surface. The deepest grooves existed and accompanied plastic deformation on the friction surface as lubricated by base oil without $MoSe_2/MoO_x$. However, flat and mild grooves accompanied occurred on the friction surfaces by the base oil with 1.0 wt% $MoSe_2/MoO_x$.

From the above results, appropriate amount of $MoSe_2/MoO_x$ heterogeneous nanostructures as lubrication additive could enhance tribological performances of the base oil. This may be due to the fact that the $MoSe_2/MoO_x$ heterogeneous nanostructures is well adsorbed and deposited on the surface of steel/steel friction pair, forming a tribofilm with low shear strength and avoiding the direct contact of the friction surface. At the same time, nanoparticles participate has a complex tribochemical reaction with surrounding elements under the action of friction, forming a tribochemical reaction layer on the steel surface, as shown in Fig. 6.

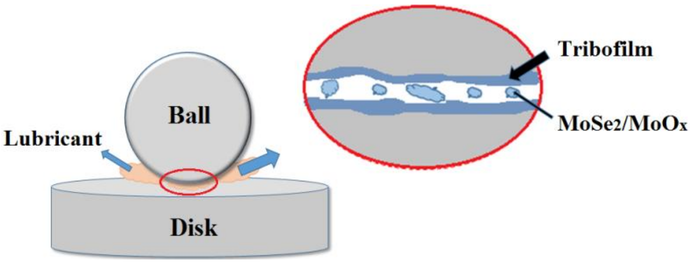

Fig. 6. Schematic diagram of friction reducing and antiwear properties between friction surfaces in the base oil with $MoSe_2/MoO_x$ heterogeneous nanostructures.

4. Conclusions

In summary, $MoSe_2/MoO_x$ heterogeneous nanostructures have been successfully synthesized via solvothermal reaction followed by an annealed process in O_2/N_2 atmosphere. The experimental results reveal that the as- synthesized $MoSe_2/MoO_x$ heterogeneous nanostructures were consisted of many flower-like assemblies and aggregated laminated crisp flakes. Furthermore, preliminary tribological tests indicated that the optimum concentration (1.0 wt%) $MoSe_2/MoO_x$ nanostructures suspended in base oil exhibit excellent tribological properties. Tribological experiments suggested that the lubrication layer and tribochemical reaction films formed on the worn surface could be benefit to reducing friction and wear of steel/steel sliding contact.

Acknowledgments

This work was supported by the 333 Project of Jiangsu Province (2016-7), the Qinglan Project of Jiangsu Province (2017-15), Changzhou Sci&Tech Program (grant no. CJ20190017) and the Key Program for Research Team of Changzhou Institute of Industry Technology (grant no. ZD201813101003).

References

[1] S. Wan, A. K. Tieu, Y. Xia, H. Zhu, B. H. Tran, S. Cui, Tribology International **102**, (2016).
[2] Q. Sunqing, D. Junxiu, C. Guoxu, Lubrication Science **11**, 3 (1999).
[3] H. Xiao, S. Liu, Materials & Design **135**, (2017).
[4] X. Jia, J. Huang, Y. Li, J. Yang, H. Song, Applied Surface Science **494,** (2019).
[5] K. Gong, X. Wu, G. Zhao, X. Wang, Tribology International **110**, (2017).
[6] M. Z. Saidi, A. Pasc, C. E. Moujahid, N. Canilho, M. Badawi, C. Delgado-Sánchez, H. Akram, Journal of Colloid and Interface Science **562**, (2020).
[7] J. Guo, R. Peng, H. Du, Y. Shen, Y. Li, J. Li, G. Dong, Nanomaterials **10**, 2 (2020).
[8] Y. Li, H. Lu, Q. Liu, Tribology International **137**, (2019).
[9] M. Q. Xue, Z. P. Wang, F. Yuan, Chalcogenide Letters **14** 2, (2017).
[10] Z. Y. Xu, Y. Xu, K. H. Hu, Y. F. Xu, X. G. Hu, Tribology International **81**, (2015).
[11] Y. Huang, Y. E.Miao, J. Fu, S. Mo, C. Wei, T. Liu, Journal of Materials Chemistry A**3**, 31 (2015).
[12] L. J. Yang, Y. Q. Deng, X. F. Zhang, H. Liu, W. J. Zhou, Nanoscale **10**, 19 (2018).
[13] W. Kang, Y. Wang, D. Cao, Z. Kang, D. Sun, Journal of Alloys and Compounds **743**, (2018).
[14] M. Q. Xue, D. Q. Liu, K. Q. Han, Chalcogenide Letters **16**, 9(2019).
[15] X. Zhang, H. Xu, J. Wang, X. Ye, W. Lei, M. Xue, C. Li, Nanoscale research letters **11**, 1 (2016).
[16] X. Zhang, Y. Xue, X. Ye, H. Xu, M. Xue, Materials Research Express **4**, 11 (2017).